Supporting Information

Lattice Breathing Inhibited Layered Vanadium Oxide Ultrathin Nanobelts for Enhanced Sodium Storage

Qiulong Wei,[†,‡] Zhouyang Jiang,[†,§] Shuangshuang Tan,[‡] Qidong Li,[‡] Lei Huang,[‡] Mengyu Yan,[‡] Liang Zhou,*[,‡] Qinyou An,[‡] and Liqiang Mai*[,‡]

[‡]State Key Laboratory of Advanced Technology for Materials Synthesis and Processing, [§]School of Chemistry, Chemical Engineering and Life Science, Wuhan University of Technology, Wuhan, 430070 P. R. China

Corresponding Author

*E-mail: mlq518@whut.edu.cn

*E-mail: liangzhou@whut.edu.cn

KEYWORDS: sodium ion battery, vanadium oxide, layer structure, nanobelt, lattice breathing

Experimental Section

Materials synthesis: The V_2O_5 sol was prepared by a melt quenching process as reported previously. The Fe-VO_x nanobelts were synthesized by a hydrothermal method. Briefly, iron (III) acetylacetonate ($Fe(acac)_3$, 0.1 mmol) was dissolve into deionized water (38.5 mL) and then 15.5 mL V_2O_5 sol (0.064 mol L^{-1}) was added under stirring. After stirring one hour, the solution was transferred into a Teflon-line stainless steel autoclave and kept at 180 ºC for 48 hours. The precipitates were collected by centrifugation, washed with deionized water and ethanol repeatedly, and dispersed into deionized water for freeze-drying. Finally, the products were obtained by vacuum drying at 150 ºC for 5 hours. The VO_x nanobelts were synthesized through the same process except that the $Fe(acac)_3$ (0.1 mmol) was replaced by acetylacetone (0.3 mmol).

Materials characterization: X-ray diffraction (XRD) measurements were performed to investigate the crystallographic information using a D8 Advance X-ray diffractometer with non-monochromated Cu Kα X-ray source. Raman spectra were obtained using a Renishaw INVIA micro-Raman spectroscopy system. Fourier transformed infrared (FTIR) transmittance spectra were recorded using the 60-SXB IR spectrometer. X-ray photoelectron spectroscopy (XPS) measurements were obtained using a VG MultiLab 2000 instrument. Thermogravimetry analysis (TGA) was performed using NETZSCH-STA449c/3/G thermoanalyzer. The morphology and structure of the product were observed through field emission scanning electron microscopy (SEM, JEOL-7100F). Transmission electron microscopy (TEM) images and high-resolution transmission electron microscopy (HRTEM) images were recorded by using a JEM-2100F microscope. Inductively Coupled Plasma (ICP) test was performed on the PerkinElmer Optima 4300DV spectrometer.

Electrochemical measurements: The electrochemical properties were evaluated by assembling 2016 coin cells in an argon-filled glove box ($O_2 \leq 0.1$ ppm and $H_2O \leq 0.1$ ppm). Sodium blocks (China Energy Lithium Co., Ltd.) were used as the anode. The 1 M solution of $NaClO_4$

in ethylene carbon (EC)/propylene carbonate (PC) with a volume ratio of 1 : 1 was used as the electrolyte. The cathodes were obtained with 70% active material, 20% acetylene black, and 10% poly(tetrafluoroethylene) (PTFE). Then the mixed clay was rolled using a roller mill to form the freestanding film. Finally, the film was cut into disks with a diameter of 8 mm. The loading of the active materials was 2~3 mg cm^{-2}. Galvanostatic charge/discharge cycling was studied with a multichannel battery testing system (LAND CT2001A). Cyclic voltammetry (CV) and electrochemical impedance spectroscopy (EIS) were tested with an electrochemical workstation (Autolab PGSTAT302N).

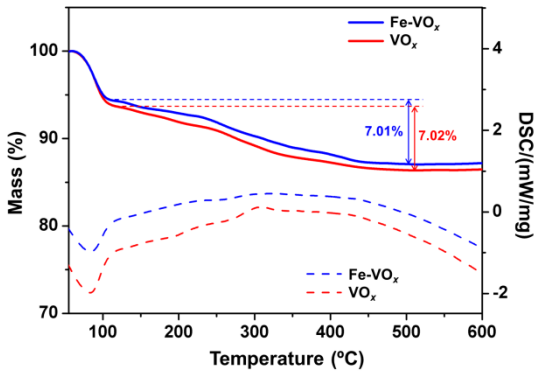

Figure S1. TG and DSC curves of the Fe-VO_x and VO_x, measured at a rate of 5 ^oC min^{-1} in N_2.

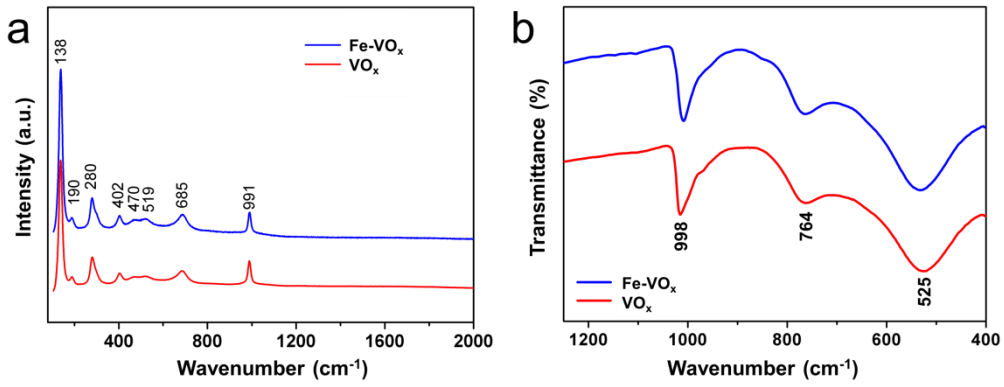

Figure S2. Raman spectra (a) and FTIR spectra (b) of the Fe-VO_x and VO_x.

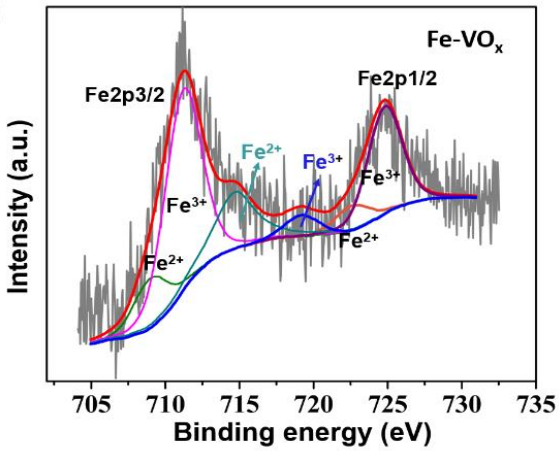

Figure S3. XPS spectrum of the Fe2p binding energy region of the Fe-VO_x. The core level binding energies of $Fe2p_{3/2}$ and $Fe2p_{1/2}$ spectra are centered at 711.25 and 724.83 eV, respectively.[1, 2] According to the previously reported results, the peak positions of Fe $2p_{3/2}$ for ferric ion (Fe^{3+}) and ferrous ion (Fe^{2+}) are located at 711.0 and 709.0 eV, and the positions of Fe $2p_{1/2}$ for Fe^{3+} and Fe^{2+} are at 724.6 and 722.6 eV, respectively. Meanwhile, two strong satellite peaks at around 719.1 and 714.78 eV originate from two typical characters of Fe^{3+} and Fe^{2+}, respectively. These results indicate that the Fe^{3+} was partially reduced to Fe^{2+} during the synthesized process. The Fe^{2+}/Fe^{3+} ratio is 0.23:1.

1. X. Zhou, G. Wu, G. Gao, J. Wang, H. Yang, J. Wu, J. Shen, B. Zhou and Z. Zhang, *J. Phys. Chem. C*, 2012, **116**, 21685-21692.
2. Q. An, F. Lv, Q. Liu, C. Han, K. Zhao, J. Sheng, Q. Wei, M. Yan and L. Mai, *Nano Lett.*, 2014, **14**, 6250-6256.

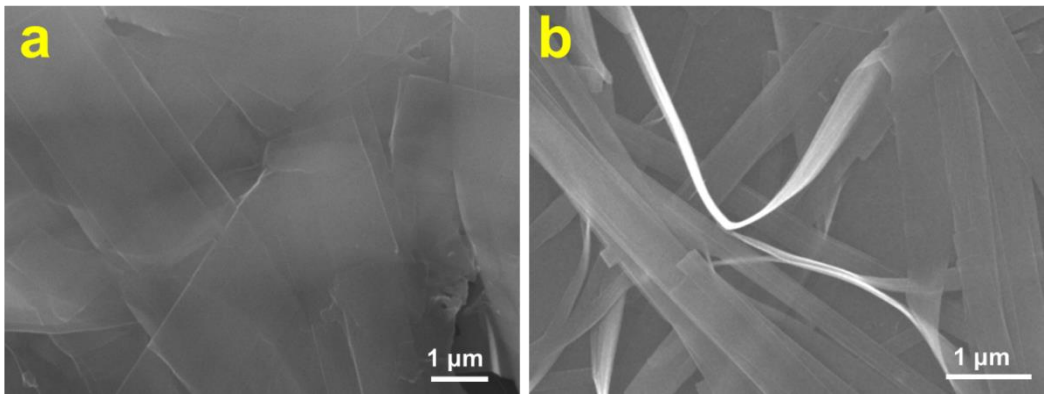

Figure S4. SEM images of the VO_x nanobelts (a) and Fe-VO_x nanobelts (b).

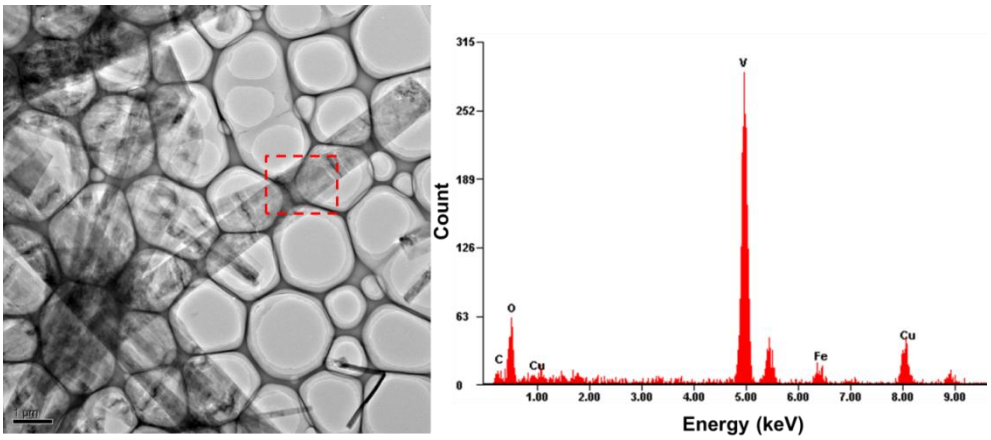

Figure S5. EDS spectrum of the Fe-VO_x nanobelt.

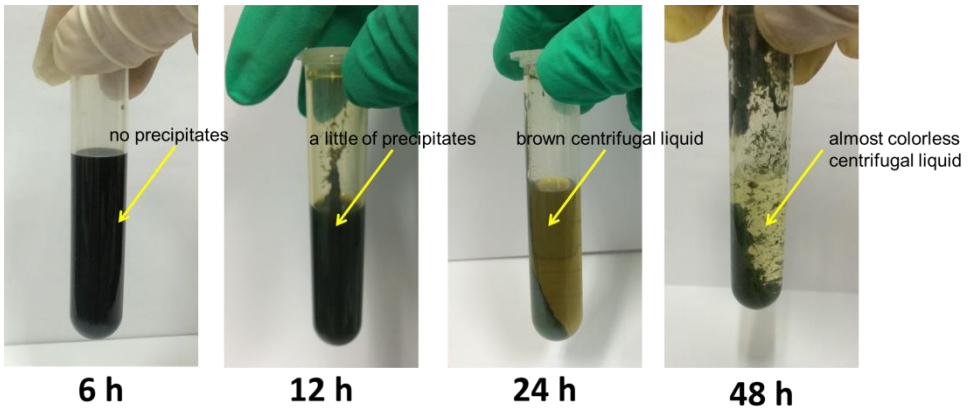

Figure S6. The optical images of the samples after different reaction times. The supernatant tends to more transparency with the increase of reaction time, indicating a more complete reaction.

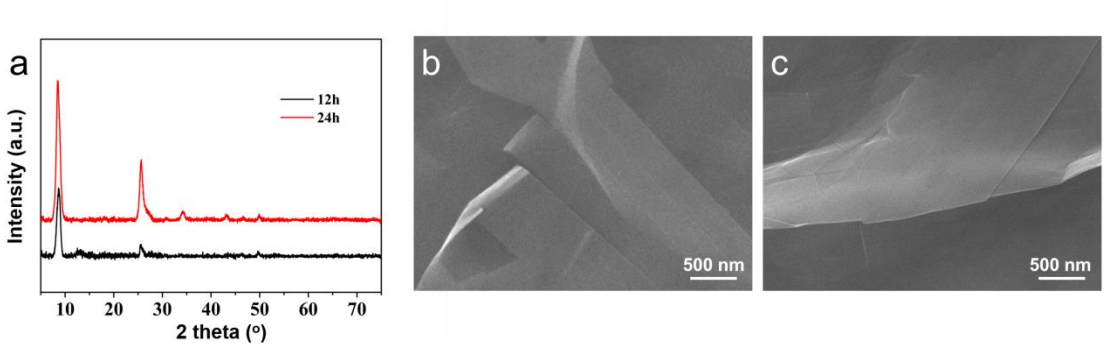

Figure S7. (a) XRD patterns of the Fe-VO_x samples after 12 and 24 hours reaction. (b,c) SEM images of the Fe-VO_x samples after 12 hours (b) and 24 hours (c) reaction, respectively.

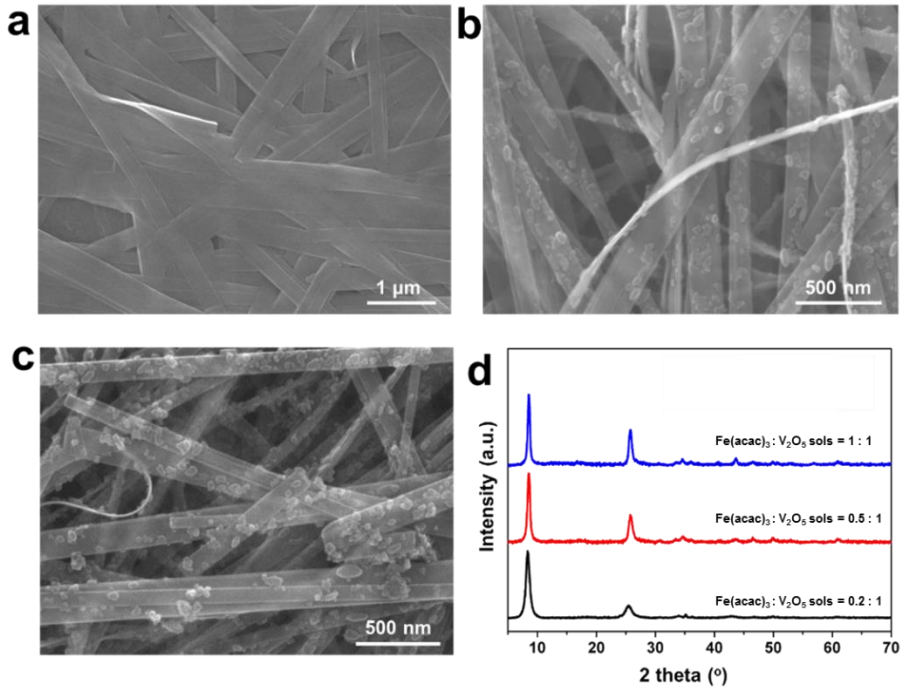

Figure S8. SEM images of the samples with more adding $Fe(acac)_3/V_2O_5$ sols ratio. (a) $Fe(acac)_3/V_2O_5$ sols = 0.2:1.0, (b) $Fe(acac)_3/V_2O_5$ sols = 0.5:1.0, and (c) $Fe(acac)_3/V_2O_5$ sols = 1.0:1.0. (d) The XRD patterns of the three samples.

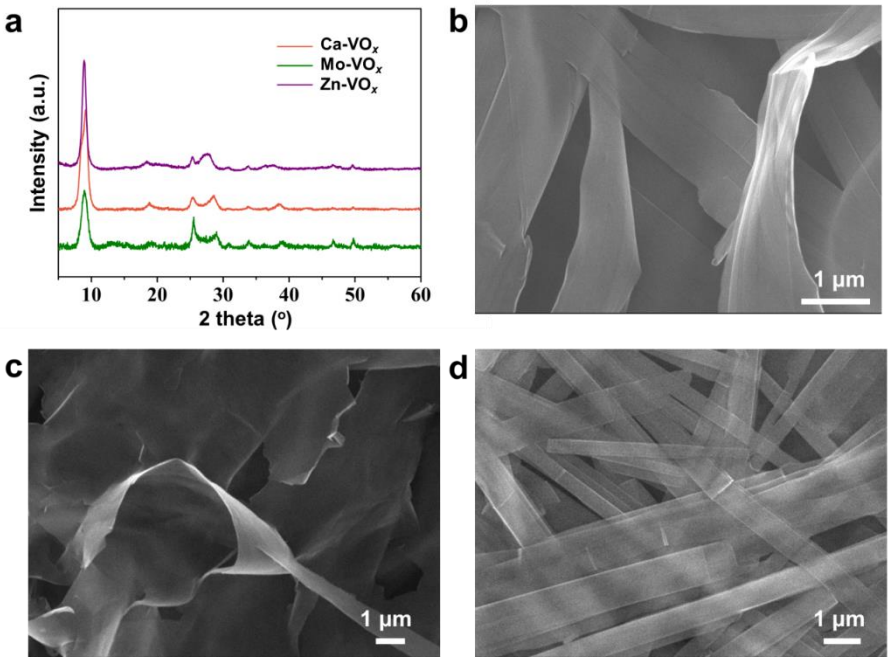

Figure S9. XRD patterns (a) and SEM images of the Ca-VO_x (b), Mo-VO_x (c) and Zn-VO_x (d) nanobelts.

Table S1. The Fe:V ratio of the Fe-VO_x and the cathode at various state from ICP analysis.

sample	Fe (wt%)	V (wt%)	Fe/V (atomic ratio)
Fe-VO_x	3.34	53.27	0.058
Fe-VO_x (first discharge at 1.0 V)	1.44	21.62	0.060
Fe-VO_x (first charge at 4.0 V)	1.756	26.05	0.061
Fe-VO_x (after 30 cycles at 4.0 V)	1.770	26.18	0.061

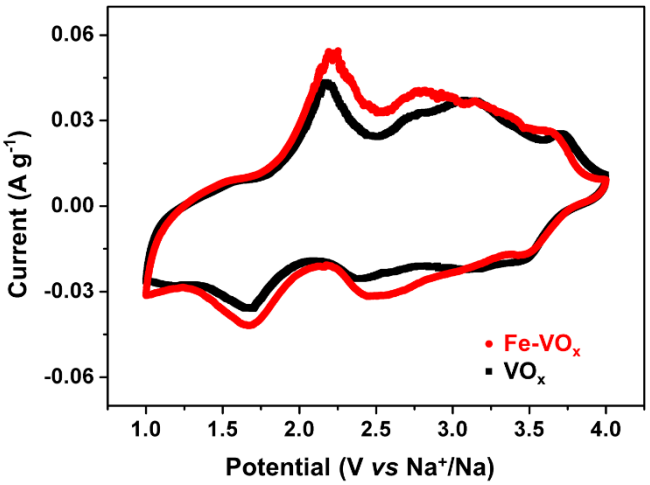

Figure S10. CV curves of the Fe-VO_x and VO_x at a scan rate of 0.1 mV s^{-1} in 1.0-4.0 V.

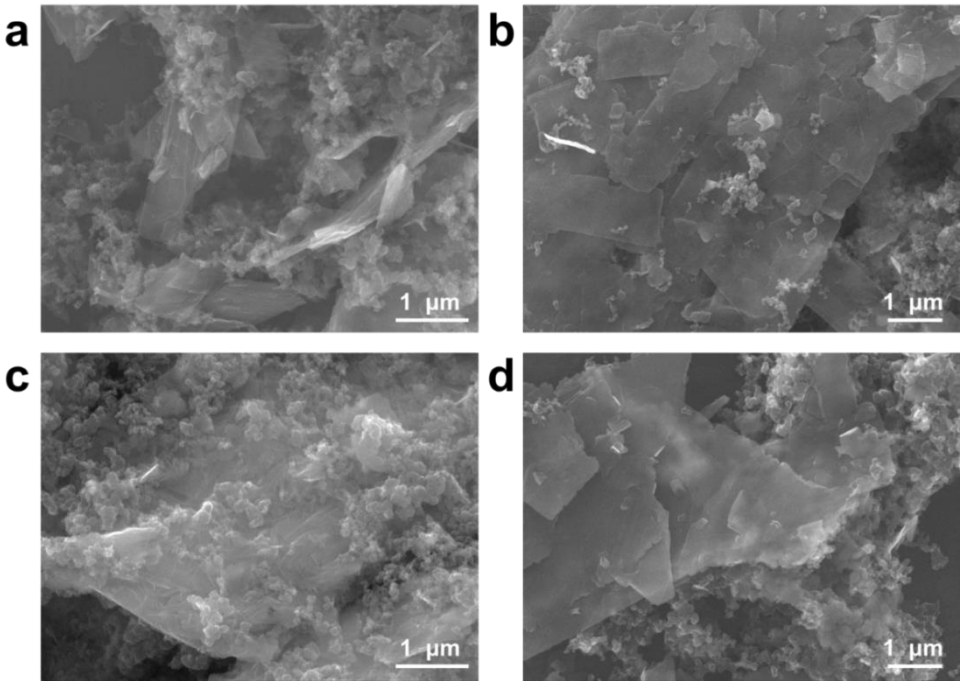

Figure S11. SEM images of the cathodes at different cycle states. SEM images of the Fe-VO_x nanobelts after first discharge to 1.0 V (a) and after 30 cycles at charged state (b). SEM images of the VO_x nanobelts after first discharge to 1.0 V (c) and after 30 cycles at charged state (d).